Oral Boldine Administration Attenuates Glia Activation and Prevents Neuropathic Pain in a Murine Spared Nerve Injury Model

Jiangping Pan [1], Yorley Duarte [2,3], Christine Chow [1], Carlos A. Toro [1, 3], Juan C. Sáez [3], Christopher P. Cardozo [1, 4, 5], Wei Zhao [1, 4*]

[1] Spinal Cord Damage Research Center, James J. Peters Veteran Affairs Medical Center, Bronx, NY, United States.

[2] Center for Bioinformatics and Integrative Biology, Facultad de Ciencias de la Vida, Universidad Andrés Bello, Santiago, Chile.

[3] Institute of Neuroscience, Centro Interdisciplinario de Neurociencia De Valparaíso, Universidad de Valparaíso, Valparaíso, Chile.

[4] Department of Medicine, Icahn School of Medicine at Mount Sinai, New York, NY, United States.

[5] Department of Rehabilitative Medicine, Icahn School of Medicine at Mount Sinai, New York, NY, United States

*** Correspondence:**

Wei Zhao, PhD

James J. Peters Veteran Affairs Medical Center

130 West Kingsbridge Road

Bronx, NY 10468, USA

wei.zhao@mssm.edu

Keywords: neuropathic pain, nerve injury, nutraceuticals, microglia, astrocyte, inflammation.

Abstract

Chronic pain is present in about 20% of the population and is a major burden to the health care system. About 30-40% of these patients report neuropathic pain. Neuropathic pain is defined as

pain caused by injury or disease of the somatosensory nervous system. Current available treatments for neuropathic pain have limited efficacy and substantial side effects. To address the need for more effective and safer treatments for neuropathic pain, this study aimed to test whether boldine, a naturally occurring alkaloid, could attenuate neuropathic pain in a murine model of spared nerve injury (SNI). We found that oral administration of boldine at 50 mg/kg body weight/day resulted in significant reduction of SNI-induced mechanical and thermal hypersensitivity. Boldine also corrected SNI-induced weight bearing deficits, which are an indication of spontaneous pain. Boldine significantly inhibited SNI-induced peripheral inflammation as indicated by reduced levels of inflammatory cytokines/chemokines in the serum. Immunofluorescence studies revealed that boldine reduced the number of reactive astrocytes and inhibited microglia activation in the dorsal horn of lumbar spinal cord. Boldine also reduced the mRNA level of pro-inflammatory markers including IL-1β and TNF-α in the lumbar spinal cord after SNI. Quantitative PCR showed that boldine inhibited the lipopolysaccharide-induced overexpression of inflammatory markers in primary mouse astrocytes and in BV-2 microglial cells. Our findings suggest that boldine may be a promising therapeutic candidate for the treatment of neuropathic pain, possibly through inhibition of glia activation and neuroinflammation.

Introduction

As described by the International Association for the Study of Pain, neuropathic pain is “pain caused by a lesion or a disease of the somatosensory nervous system". It affects 7-10% of the general population globally [1]. Neuropathic pain can be central or peripheral, and tissue damage is not always apparent. Studies have shown that neuropathic pain has multiple adverse effects in both humans and rodents that include impaired sleep, depression, anxiety, and lower quality of life [2-5]. Common causes of neuropathic pain include trigeminal neuralgia, post-amputation pain, persistent post-operative or post-traumatic pain, pain after peripheral nerve injury, painful diabetic neuropathy, cancer pain, and chemotherapy-induced peripheral neuropathy. Due to its subjective nature, diagnosing neuropathic pain is challenging. Typical characteristics of neuropathic pain include allodynia, where normally non-painful stimuli cause pain; hyperalgesia, an exaggerated response to painful stimuli; and spontaneous pain [6-9].

Currently, the first line of choice for neuropathic pain treatment includes: anticonvulsants (e.g., gabapentin and pregabalin); tricyclic antidepressants (e.g., amitriptyline); serotonin and norepinephrine re-uptake inhibitors (e.g., duloxetine) and topical agents (e.g., lidocaine patches or creams, capsaicin creams) [10]. When first-line treatments do not provide sufficient relief or are not well-tolerated, N-methyl-D-aspartate (NMDA) receptor antagonists (e.g., ketamine), may be

considered as an alternative option in specific cases including central neuropathic pain and neuropathic pain in cancer. Opioids, such as morphine and oxycodone, can be administered under careful medical supervision for very severe cases, although their long-term efficacy in treating neuropathic pain is uncertain, and they can be associated with severe side effects and risks, including sedation, respiratory depression, constipation, nausea, itching, hormonal effects, and potential dependence and addiction [11]. Thus, there is an urgent need to develop novel, efficacious and safe interventions for treating neuropathic pain. Recently, the beneficial effect of some nutraceuticals (dietary supplements and herbal/natural products) including Vitamin B, Vitamin D, zinc, magnesium, and herbal remedies have gained attention in combating neuropathic pain [12]. Curcumin for instance, reduced neuropathic pain in streptozotocin-induced diabetic neuropathy [13] and peripheral nerve injury rodent models [14].

Boldine is the most abundant alkaloid isolated from the leaves and bark from boldo (*Peumus boldus*), a widely distributed evergreen tree native to Chile [15]. Boldo extracts containing boldine has been used since the last century in Europe and North/South America, for the treatment of digestive problems, headache, rheumatism and urinary tract inflammation [16]. Boldine has also been shown to have antioxidative activities that protect both biological and non-biological systems against free radical-mediated oxidative damage [17]. In addition, boldine exhibits hepatoprotective, anti-inflammatory and antipyretic activities in animal models [18, 19]. Recent studies conducted by us and others have shown the beneficial effect of boldine in neurological conditions including spinal cord injury [20, 21], delayed nerve repair [22] and Alzheimer's Disease [23], suggesting that boldine could pass the blood-brain barrier. Consistent with this interpretation, boldine accumulates in brain tissues after oral administration [24]. Considering the anti-inflammatory activity of boldine and the key role of neuroinflammation in the development and maintenance of neuropathic pain, we administered boldine to a mouse model of spared nerve injury and evaluated its potential to attenuate neuropathic pain.

Material and Methods

Animal, Surgery, and Boldine Administration

All animals were maintained on a 12:12-h light/dark cycle in a temperature-controlled (20 ± 2°C) vivarium, with food and water *ad libitum*. All procedures were approved by the Institutional Animal Care and Use Committee at James J. Peters Veterans Affairs Medical Center and conformed to all guidelines and regulations for the protection of the welfare of animals. 8-10 weeks old female C57BL6 mice were purchased from the Jackson Laboratory (Bar Harbor, ME). Spared

nerve injury (SNI) surgery was conducted on the left hindlimb under anesthesia (3-5% isoflurane). Briefly, about 3-cm long blunt dissection was made into the skin overlying the area between the gluteus and biceps femoris muscles, and the common sciatic nerve of the hind paw was exposed at the mid-thigh level. Peroneal and tibial nerves were cut, leaving an intact sural nerve. The skin was closed using the Reflex 7 mm wound clips. Sham animals underwent a similar procedure where the branches of the sciatic nerve were exposed but left intact. Boldine (Sigma-Aldrich, St. Louis, MO) was administered to the animal right after surgery via a customized chow (Research Diets, New Brunswick, NJ) to reach a dose of 50 mg/kg/day. A control diet (OpenStandard Diet With 15 Kcal% Fat, Research Diets) was provided to sham-operated or SNI group. Mice were then allowed to recover from surgery for at least 24 hours before pain phenotype testing began. Animals were euthanized at 15 days post-surgery. Blood and lumbar spinal cord (L3-5) were collected and stored at -80°C for further analysis.

Behavioral Tests

Mechanical pain responses were assessed by Von Frey filament test performed on the ipsilateral and contralateral hind paws [25]. Briefly, animals were placed on an elevated platform with a surface of wire mesh. The Von Frey hair (Bioseb, Vitrolles, France) is then inserted perpendicularly from below the platform, up through the wire mesh and into the plantar surface of the hind paw, starting with the smallest gauge filament. The pressure was increased slowly, until the hair just began to bend. The test was then repeated with the next largest gauge filament until withdrawal responses including paw flicking, paw lifting, paw licking or possibly vocalizing were observed. The withdrawal threshold, defined as the smallest gauge wire that produced a withdrawal response, was recorded.

Thermal pain responses were measured using a hot/cold pate apparatus (Maze Engineers, Skokie, IL). Mice were allowed to move freely on a hot/cold plate enclosure for a maximum of 30 seconds. For assessing pain responses to heat, plate temperature was set at 50˚C. For testing pain responses to cold, plate temperature was set at 15˚C. Once paw retraction, paw licking, or escaping behaviors were observed, mice were immediately taken out of the testing apparatus and the time latency was recorded [26].

Spontaneous pain responses were measured using the Dynamic Weight Bearing 2.0 system (DWB2.0) (Bioseb, Vitrolles, France) as described [27]. Briefly, the animal was placed into the DWB enclosure for a test duration of approximately 5 minutes. A matrix comprising around 2000 high precision force sensors (0.02 g for mice), embedded in the floor of the enclosure where the animal is free to move, measures the weight distribution on each of the four paws of the animal. The animal was filmed from above using a high-definition camera and the

captured video feed was analyzed in real-time using tracking software which allows a precise analysis of the animal's posture. An observer manually validated each automatically presumed paw position to avoid subsequent error identification afterward.

Multiplex ELISA

MILLIPLEX® Mouse Cytokine/Chemokine Magnetic Bead Panel (Millipore, Billerica, MA) was used to measure the levels of 32 cytokines/chemokines in mouse serum as previously described [28-30]. Briefly, 25 µl of serum sample was diluted with assay buffer and incubated with magnetic beads overnight at 4°C. The samples were then washed, incubated with detection antibodies for 1 hour at room temperature followed by streptavidin-phycoerythrin incubation for 30 minutes. The plate was run on a Luminex 200 instrument (Millipore, Billerica, MA) and the median fluorescent intensity was used to calculate the concentration of each cytokine/chemokine.

Immunostaining and microscopy

At 15 days post injury, mice were transcardially perfused with saline followed by 4% paraformaldehyde (PFA). Lumbar spinal cords (L3-5) were harvested and transversely sectioned using a LEICA CM3050 S Cryostat (LEICA, Wetzlar, Germany). For immunostaining, slides were first blocked in blocking buffer (1xPBS+5% goat serum+0.3% Triton X-100) for 1h at room temperature, then incubated with primary antibodies of astrocyte marker glial fibrillary acidic protein (GFAP, 1:200, Abcam, Cambridge, United Kingdom) or activated microglia marker major histocompatibility complex II (MHC II, 1:200, Abcam) overnight at 4°C. After incubation, the slides were washed in PBS for 3 times and incubated with goat anti-mouse Alexa Fluor 488 secondary antibody (1:250, Abcam) for 1 hour at room temperature. Slides were then washed with PBS three times and mounted with VECTASHIELD Antifade Mounting Medium (Vector Laboratories, Newark, CA). Images were acquired using the ZEISS LSM 700 confocal imaging system (Carl Zeiss AG, Oberkochen, Germany) with 20× objective.

Cell culture and treatment

All the cell incubations were performed at 37°C, 5% CO_2 and 95% relative humidity. BV-2 cells (murine microglial) were maintained in Dulbecco's Modified Eagle Medium (DMEM) (GIBCO) supplemented with 10% fetal bovine serum (FBS, GIBCO) and antibiotics (penicillin 100 U/ml, streptomycin 100 µg/ml, GIBCO). Primary spinal cord astrocytes were generated from P2 C57BL6 mice as described [20, 31]. Briefly, dissociated cells were resuspended in DMEM with 10% FBS, transferred to poly-L-lysine coated flask, and incubated for 24 h to allow adhering. Flasks were then shaken at 200 rpm at 37°C overnight. The following day, non-adherent oligodendrocytes, neurons, and microglial were removed and the remaining adherent cells were gently washed once with DMEM containing 10% FBS. Cells were then allowed to recover and proliferate for 10 days

before treatment. Cells (in triplicates) were stimulated with 100 ng/ml lipopolysaccharides (LPS, Sigma-Aldrich) with or without boldine (25 μg/ml or 50 μg/ml) for 6 h, and 100 μl of the supernatant was sampled for cytotoxicity essay before cells were harvested for RNA extraction or ELISA.

Cytotoxicity assay and ELISA

Cell viability was assessed using the CytoTox 96® Non-Radioactive Cytotoxicity Assay (Promega, Madison, WI). For ELISA assay, BV-2 cells were harvested and lysed in RIPA buffer (Pierce Biotechnology, Waltham, MA). Protein concentration was measured using the BCA Protein Assay Kits (Pierce Biotechnology). IL-1β protein levels were assessed using the Mouse IL-1 beta/IL-1F2 Quantikine ELISA Kit (R&D Systems, Minneapolis, MN) following the manufacturer's directions. Optical density at 450 nm was read on a multimodal microtiter plate reader (SpectraMax iD5, Molecular Devices, San Jose, CA).

RNA Isolation, cDNA synthesis and Quantitative PCR

BV-2 cells and primary mouse astrocytes were harvested and RNAs were extracted using the RNeasy Kit (Qiagen, Hilden, Germany) following the manufacturer's directions. Frozen tissues were homogenized in TRI-Reagent (Sigma-Aldrich, St. Louis, MO) using a FastPrep-24™ 5G Bead Beating Grinder and Lysis System (MP Biomedicals, Solon, Ohio). Total RNA was isolated following the manufacturer's instructions. RNA concentrations were measured using a NanoDrop Spectrophotometer (Thermo Fisher Scientific, Waltham, MA). One microgram of total RNA was reverse transcribed with High-Capacity cDNA Reverse Transcription Kit (Applied Biosystems) using random hexamers in a 20 μl reaction according to the manufacturer's protocol. Quantitative PCR (qPCR) was performed using the Taqman Universal PCR Master Mix (Applied Biosystems, Waltham, MA) on a ViiA 7 Real-Time PCR System (Applied Biosystems, Waltham, MA). Relative expression levels were calculated using the $2^{-\Delta\Delta Ct}$ method with hypoxanthine phosphoribosyltransferase 1 (HPRT) as an internal control. A list of the Taqman probes used in this study are provided in Supplemental Table 1 (all from Applied Biosystems).

Molecular docking and dynamics studies

Human connexin-43 electron microscopy structure (PDB ID: 7F92) was used for the *in silico* experiments focusing on previously identified D4 and valproic acid binding site [32]. Interaction between boldine and the binding site was evaluated with the Glide software [33] in Schrödinger Suite (Release 2023-3, Schrödinger LLC, New York, NY) using the software's default settings to ensure uniformity and reproducibility. The structure of boldine was obtained from PubChem in its two-dimensional form, and the LigPrep suite was used to prepare it for analysis. The docking analysis was conducted in standard precision mode, which provided a flexible sampling of the

ligand conformations. The Glide Docking Score algorithm was used to assess and score the produced poses, with its default settings. The binding site was identified as druggable because of its affinity for interacting with the ligand, and conformations that showed the highest favourable docking scores were selected. Brief molecular dynamic simulation was performed using Desmond software from the Schrödinger suite as previously described [34]. The Simulation Interaction Diagram tool of Schrödinger's Maestro platform was used to analyse the generated molecular dynamic data. Subsequently, the binding free energy of the connexin-43-boldine complexes was estimated using the Molecular Mechanics-Generalized Born Surface Area MM-GBSA approach.

Statistical analysis

Data were analyzed using GraphPad Prism 10 and were presented as the mean ± standard error of the mean (SEM). Two-way repeated-measures analysis of variance (ANOVA) followed by multiple comparison test were performed to compare the mean differences in mechanical thresholds, thermal thresholds and weight bearing between the experimental groups. One-way ANOVA followed by multiple comparison test was performed for the comparison of mean difference in cytotoxicity and RNA or protein expression levels between the experimental groups. p-value of <0.05 was considered statistically significant.

Results

Boldine prevented SNI-induced mechanical allodynia. There are several well-accepted animal models for the study of peripheral nerve injury-induced neuropathic pain, including chronic constriction injury (CCI) of the sciatic nerve, partial sciatic nerve ligation, spinal nerve ligation, spared nerve injury (SNI), brachial plexus avulsion, and sciatic nerve transection [35]. The SNI model is achieved by complete transection of the common peroneal and tibial nerve branches of the sciatic nerve, leaving an intact sural nerve [36]. SNI model produces persistent peripheral hypersensitivity to mechanical stimuli. To assess the role of boldine in peripheral nerve injury-induced neuropathic pain, we conducted studies in a mouse model of SNI. Briefly, 8-10 weeks old female C57BL6 mice were subjected to SNI surgery or sham surgery. A customized diet containing boldine or control diet (all from Research Diets) was administered right after surgery. Pain phenotyping tests including Von Frey filament test, hot/cold plate test and dynamic weight bearing test were performed starting from 3 days after injury. As expected, SNI significantly induced mechanical pain hypersensitivity on the ipsilateral hindlimb at 3-, 7-, and 14 days post injury (Fig. 1A, $p<0.001$) when compared to sham-operated animals. Oral administration of boldine completed prevented this injury-induced mechanical allodynia (Fig. 1A, $p<0.001$, SNI+boldine vs. SNI). There was no change of responses to mechanical stimuli after nerve injury

or boldine treatment on the contralateral hind limb (Fig. 1B), suggesting that the boldine-mediated alleviation of mechanical allodynia is specific to the region innervated by the injured nerve.

Boldine reduced SNI-induced thermal pain. Studies using the SNI model have demonstrated alterations in thermal pain sensitivity. Specifically, rodents with SNI often exhibit increased sensitivity to thermal stimuli, manifesting as decreased withdrawal latencies in response to heat or cold compared to control animals [36]. To test the effect of boldine in altering thermal pain phenotypes, we performed the hot plate test and the cold plate test using a hot/cold plate apparatus (Maze Engineers, Skokie, Illinois). At 7 days post injury, SNI animals developed an increased sensitivity to both warm (Fig. 1C, $p<0.001$ SNI vs. sham) and cold stimuli (Fig. 1D, $p<0.01$ SNI vs. sham). Administration of boldine significantly attenuated the SNI-induced-hypersensitivities to hot (Fig. 1C, $p<0.01$ SNI+boldine vs. SNI) and cold (Fig. 1D, $p<0.05$, SNI+boldine vs. SNI) temperatures.

Boldine prevented some SNI-induced weight bearing changes. Weight bearing is an important aspect of motor function and mobility, and alterations in weight-bearing behavior can be indicative of pain or motor deficits, including those resulting from peripheral nerve injury. In the context of SNI, changes in weight-bearing distribution are often observed as part of the pain-related behavioral phenotype [37]. To evaluate the effect of boldine on potential SNI-induced weight bearing deficits, we performed weight bearing tests using the dynamic weight bearing 2.0 system (DWB 2.0). As compared to sham-operated mice, injured mice tended to use the ipsilateral hindlimb less for weight support at 3- and 7-days post injury (Fig. 2A, $p<0.001$), and boldine administration significantly alleviated the SNI-induced weight bearing deficit at 7dpi (Fig. 2A, $p<0.05$). Using the DWB2.0 system, we also measured some other parameters including the hindlimb weight support area ratio, rearing duration and hindlimb posed duration. SNI led to significantly decreased ipsilateral weight support area (Fig. 2B) and markedly lower rearing duration (Fig. 2C). However, administration of boldine did not prevent SNI-induced deficits in weight support area or rearing duration. There is a trend toward a decrease of the posed duration on the ipsilateral hindpaw after injury although it did not reach out threshold for statistical significance (Fig. 2D).

Boldine reduced peripheral inflammation after SNI. Boldine has been shown to exhibit anti-inflammatory activities [18, 19]. To evaluate the effect of boldine on peripheral inflammation, blood samples were collected at 15 days post injury (dpi) and subjected to a multiplex ELISA using the MILLIPLEX® Mouse Cytokine/Chemokine Magnetic Bead Panel (Millipore). Significantly increased levels of cytokines and chemokines including Interleukin-12 (IL-12p40), Interleukin-15

(IL-15), macrophage colony-stimulating factor (M-CSF) and chemokine ligand 5 (CCL5) were detected in serum after injury (Fig. 3). We also noticed trends of increase for some other cytokines/chemokines including IL-1β, IL-5, IL-9, and C-X-C motif chemokine ligand 9 (CXCL9), although no statistical significance was found. Boldine treatment decreased the expression of the above-mentioned inflammatory markers (Fig. 3) in the serum, suggesting that boldine could reduce SNI-induced peripheral inflammation.

Boldine inhibited glia activation in the lumbar spinal cord dorsal horn. In pain conditions, nociceptive signals are transmitted from peripheral nerves to the spinal cord. The spinal cord dorsal horn plays a crucial role in processing pain signals. These signals then ascend to the brain for further processing and interpretation. Glial cells in the spinal cord dorsal horn play complex and dynamic roles in pain processing. Their activation and interactions with neurons contribute to the amplification and maintenance of pain signals, as well as the development of chronic pain. Both activated microglia and reactive astrocytes have been implicated in pathogenesis of pain following nerve injuries [38-42].To test the effect of boldine on glia activation, transverse lumbar spinal cord sections collected at 15 dpi were immuno-stained with the astrocyte marker GFAP (Abcam) or the activated microglia marker MHC II (Abcam). As compared to sham-operated mice, significantly more reactive astrocytes were detected in the dorsal horn of lumbar spinal cord after SNI, and boldine treatment reduced the number of GFAP-positive cells (Fig. 4, top panel). As expected, there were almost no MHC II-positive cells detected in the spinal cord of sham-operated mice. After injury, microglia in the spinal cord were activated as shown by strong MHC II-positive signals and boldine treatment completely prevented the SNI-induced microglia activation (Fig. 4, bottom panel).

Boldine reduced neuroinflammation in the spinal cord. Glia mediators, such as IL-1β and tumor necrosis factor-α (TNF-α), are key factors in the glial control of pain. IL-1β is induced in astrocytes and microglia in the spinal cord after nerve injury [43]. Inhibition of IL-1β signaling reduces inflammatory, neuropathic and cancer pain [44]. It has been reported that overexpression of IL-1β in the injured sciatic nerve following nerve injury may be a common mechanism underlying the generation of neuropathic pain [45]. C–C motif chemokine ligand 2 (CCL2), also known as monocyte chemotactic protein 1 (MCP-1), and its receptor CCR2 may play a role in neuroinflammation by participating in neuron-glial cell interactions [46-48]. To evaluate the effect of boldine on these inflammatory markers in the lumbar spinal cord following SNI, we extracted RNA from lumbar spinal cord collected at 15 dpi and performed quantitative PCR using the standard Taqman method. We found significantly elevated levels of TNF-α ($p<0.001$, Fig. 5A) and

CCL2 ($p<0.05$, Fig. 5B) mRNA in the lumbar spinal cord following SNI. A trend of increased IL-1β expression was also detected, although it did not reach statistical significance ($p=0.0569$, Fig. 5C). Oral administration of boldine decreased the expression of TNF-α ($p<0.05$, Fig. 5A) and IL-1β ($p<0.05$, Fig. 5C) in the spinal cord following SNI. A trend of decrease in CCL2 mRNA level is also noted, although it did not reach statistical significance (Fig. 5B).

Boldine inhibited inflammation in glial cells. To dissect the potential underlying mechanism of boldine action in glial cells, BV2 microglia cells were treated with 100 ng/ml lipopolysaccharide (LPS) with or without boldine (25 μg/ml or 50 μg/ml) for 6 hours. After treatment, cell medium was collected and subjected to a cell viability assay. Neither the 25 μg/ml or the 50 μg/ml dose of boldine showed any cytotoxicity (Supplemental Figure 1A). Cells were then harvested and subjected to analysis of mRNA levels by quantitative PCR. LPS treatment led to significantly elevated mRNA levels of chemokines (CCL2, CCL3 and CCL5), cytokines (IL-1β, IL-6, IL-18 and TNF-α), macrophage and microglia marker CD11b, toll-like receptors (e.g. TLR2 and TLR3), NOD-, LRR- and pyrin domain-containing protein 3 (NLRP3), and caspase1 (Fig.6). Co-incubation with 25 μg/ml or 50 μg/ml boldine inhibited the LPS-induced upregulation of CCL2, CCL3, CCL5, IL-1β, IL-6, IL-18, CD11b, TLR2, TLR3, NLRP3 and caspase1. IL-1β protein levels in the cell lysates were also measured by ELISA. IL-1β protein levels were drastically increased after LPS treatment, and boldine significantly reduced IL-1β protein level in a concentration-dependent manner ($p<0.001$, Supplemental Figure 1B). Similarly, we found that boldine significantly decreased LPS-induced upregulation of CCL2, IL-1β, IL-6, TLR2, TLR3, TLR6, NLRP3, caspase1 and nuclear factor-kappa B (NFκB) mRNA levels (Fig. 7) in primary mouse astrocytes. Collectively, our *in vitro* and *in vivo* results suggested that boldine might reduce neuropathic pain through inhibiting neuroinflammation pathways. Further studies are still needed to explore the direct target of boldine.

In silico binding of boldine to connexin-43 hemichannel. It has been reported that connexin hemichannels could mediate neuroinflammation in multiple disease conditions [49]. We and others have reported blockade of glial hemichannels by boldine in cultured cells [20, 50]. Previously, we reported that the compound D4 mitigates neuroinflammation by inhibiting connexin-43 hemichannel. Molecular structural analysis revealed that D4 binds to a specific domain within the connexin-43 hemichannel. This domain includes the N-terminal helix (NTH), transmembrane helix 1 (TMH1), and TMH2 of one protomer, alongside TMH1 from an adjacent protomer located beneath the NTH [34, 51]. The binding potential of boldine at the predicted connexin-43 hemichannel binding site was studied using the molecular docking approach. Our

findings revealed that the binding interactions for boldine mirrored those observed for D4, suggesting that boldine may also anchor within a similar domain encompassed by the NTH, TMH1, and TMH2 across two protomers [34]. Boldine appeared to be in the cytoplasmic and transmembrane areas of connexin-43 hemichannel (Supplemental Figure 2A). Notably, a hydrophobic pocket appears to facilitate the accommodation of boldine through π-stacking, cation-π, and van der Waals forces, engaging with Phe97 in TMH2, Trp4 in the NTH, Val28 in TMH1, and Leu93 in TMH2 (Supplemental Figure 2B-C). Our molecular dynamics simulations confirmed that boldine is stable within the connexin-43 hemichannel predicted binding site. By measuring binding energy during the last simulation time using the MM-GBSA approach, we observed a considerable binding energy of -62.7 ± 2.9 kcal/mol. The main contributors of this energy were lipophilic interactions and van der Waals forces.

Discussion

The SNI model is a commonly used model in rodents to study neuropathic pain. SNI leads to mechanical allodynia, which develops 3 days after injury and lasts between 4 weeks to 12 months in mice [52]. SNI also leads to thermal hypersensitivity and weight bearing deficits. In this study, we found that oral consumption of boldine could prevent SNI-induced mechanical allodynia at 3-, 7-, and 14 dpi. Boldine also prevented SNI-induced thermal hypersensitivity and weight bearing deficit at 7 days post injury. However, we notice that animals start to recover from thermal or weight bearing pain responses at 14 dpi, which is consistent with previous report that thermal hypersensitivity and weight bearing share similar pain recovery profiles, whereas mechanical allodynia persists [53]. Rearing behavior, where a mouse stands on its hind legs with its forelimbs raising and head extending, has been used as a spontaneous pain indicator in mice [54]. We found significantly decreased rearing duration after SNI. However, boldine treatment did not improve rearing duration. Further experiments using boldine for longer period could evaluate its efficacy to prevent chronic pain development. In addition, administering boldine at a later time point after nerve injury could also be performed to evaluate the potential of boldine to alleviate existing neuropathic pain.

Neuroglial cells, including microglia, astrocytes, oligodendrocytes, and ependymal cells, play complex and dynamic roles in pain processing. Their activation and interactions with neurons contribute to the amplification and maintenance of pain signals, as well as the development of chronic pain conditions [55]. After tissue damage, neurons are assisted by glial cells that are activated at the dorsal root ganglia and the dorsal horns of the spinal cord [56]. Microglia, comprising ~10-15% of all glial cells, are a specialized population of mononuclear macrophages

located in the central nervous system (CNS) [41]. After nerve damage, microglial cells in the spinal cord undergo morphological changes (ramified, rod-like, activated and amoeboid microglia) [57], and increase in number. Our immunofluorescence data confirmed increased number of reactive astrocytes and activated microglia following nerve injury. Importantly, boldine treatment at 50 mg/kg BW/day significantly attenuated/blunted/alleviated the injury-induced glia activation. Further studies on quantifying the morphological changes of microglia after nerve damage and boldine treatment will provide a better understanding of how boldine inhibits microglia activation.

Inflammatory responses are of great significance in the development of neuropathic pain. A large body of evidence indicates that inflammatory mediators (e.g., proinflammatory cytokines) in local inflamed tissues, peripheral nerves, and spinal cord make important contributions to the initiation and maintenance of chronic pain [58, 59]. In this study, we have demonstrated that after SNI, boldine significantly reduced the expression of pain-related inflammatory markers including IL-1β, IL-5, IL-12p40, IL-15, CCL5, CXCL9 and M-CSF in the serum. Excessive production of IL-1β has been implicated in the pathophysiology of acute or chronic inflammation and pain. IL-1β may contribute to pain via direct and indirect mechanisms, by either directly activating nociceptors to elicit action potentials and induce pain [60], or contributing to peripheral or central sensitization by sensitizing nociceptors or promoting neuron-glia crosstalk [61-63]. High levels of IL-5 have been associated with fibromyalgia and joint pain [64, 65]. Subcutaneous injection of IL-12 leads to mechanical hyperalgesia in rats [66]. IL-15 has been linked with nerve injury-induced neuropathic pain in a rodent CCI models [67] as well as rheumatoid arthritis- and osteoarthritis-induced joint pain in humans [68]. Intradermal injection of CCL5 has been shown to induce pain and administration of Met-CCL5, an antagonist of CCL5 receptor CCR5, attenuates inflammatory and nociceptive responses following peripheral nerve injury [69]. Increased CCL5 level has been found in the anterior cingulate cortex after CCI [70]. In humans, upregulated CCL5 has been detected in patients with various pain conditions including small fiber neuropathy [71], atypical facial pain and trigeminal neuralgia [72], and discogenic back pain [73, 74]. CXCL9 plays an important role in diabetic neuropathy [75] and neuropathic pain conditions [76]. M-CSF is also an important contributing factor to the development of neuropathic pain [77] and arthritic pain [78]. The boldine-mediated reduction of these pain-related inflammatory cytokines/chemokines in the blood suggests that boldine could prevent systematic inflammation after nerve injury.

In the central nervous system, glial cells express numerous receptors, including those for glutamic acid, gamma-aminobutyric acid, norepinephrine, acetylcholine, and cannabinoids that

are involved in pain signaling. Activation of these receptors leads to the release of pro-inflammatory substances, and contributing to chronic neuroinflammation [79]. In this study, we report that boldine reduced the LPS-induced overexpression of multiple inflammatory cytokines and chemokines including CCL2, IL-1β, IL-6, and IL-18 in primary mouse astrocytes and in BV-2 microglial cells. Although we did not observe any change of TNF-α mRNA after *in vitro* boldine treatment, a significant decrease of TNF-α and IL-1β mRNA in the lumbar spinal cord was detected in boldine-treated animals 15 days after nerve injury. We have also found decreased expression of toll-like receptors (e.g. TLR2, TLR3 and TLR6), NLRP3, caspase1 and NFκB after boldine treatment. Recent studies have shown that after nerve injury, toll-like receptors (TLRs) are involved in the generation of neuropathic pain. For example, TLR2 and TLR4 modulate glial activation in the spinal cord and contribute to neuropathic pain development [80, 81]. TLRs are responsible for the stimulation of astrocytes and microglia, which will induce proinflammatory mediators and cytokines, therefore leading to the generation and maintenance of neuropathic pain. The majority of TLRs can signal primarily through the myeloid differentiation 88 (MyD88) pathway, and then trigger the activation of ERK/JNK/NFκB signaling. Nod-like receptors (NLRs) are cytoplasmic sensors that oligomerize to form the inflammasome, a multi-subunit complex that processes the maturation of pro-IL-1β and pro-IL-18 via caspase-1 [82]. A well-characterized outcome of TLR and inflammasome interaction is the secretion of IL-1β and IL-18 [83]. Our data in BV-2 and primary astrocytes suggest that boldine might reduce neuroinflammation through inhibiting the TLR/NLRP3 inflammasome signaling, but the direct target of boldine still remains to be characterized.

Recent studies report that connexin hemichannels could mediate neuroinflammation in multiple disease conditions [49] and boldine could block glial connexin hemichannels in cultured cells [20, 50]. In this study, we report the *in-silico* binding of boldine to connexin-43. Several lines of evidence implicate the role of connexin 43 in the pathogenesis of neuropathic pain. For example, the connexin43 hemichannel blocker Peptide 5 inhibited NLRP3 inflammasome activation and alleviated mechanical pain hypersensitivity in nerve-injured mice [84]. Upregulated connexin-43 were detected in the spinal astrocytes after chronic constriction injury, and spinal injection of selective or non-selective hemichannel blocker could effectively reduce mechanical allodynia in this model [42]. Chronic amitriptyline treatment demonstrated anti-hyperalgesia-like effects through astroglial connexin-43 hemichannel inhibition in CCI rats [85]. Future *in vitro* receptor binding experiments and *in vivo* animal experiments using microglia-specific connexin-43

knockout mice will explore the possibility that connexin-43 hemichannel is the direct target of boldine in attenuating nerve injury-induced neuropathic pain.

Neuropathic pain involves complex interactions between neural and non-neural cells, and glial cells playing a central role in the development and maintenance of neuropathic pain. New therapeutic approaches aim to target these cells and their signaling pathways to provide effective pain relief. We report, for the first time that oral administration of boldine, an alkaloid from a Chilean tree, inhibited glia activation and attenuated neuropathic pain in a murine model of spared nerve injury, suggesting that boldine might be considered as a novel therapeutic agent for the treatment of neuropathic pain. Future studies characterizing the receptor binding activities, pharmacokinetics, *in vivo* efficacy, and underlying mechanism of boldine as well as its derivatives are needed to better define the potential for therapeutic application in afflicted patients.

Figure Legend

Fig.1 Effect of boldine in SNI-induced mechanical and thermal pain phenotypes. C57BL6 mice were subjected to spared nerve injury (SNI). Boldine was administered right after injury via a customized diet (Research Diet) to reach a dose of 50 mg/kg/day. A control diet was provided to sham or SNI group. Von Frey filament tests and hot/cold plate tests were performed to evaluate mechanical and thermal pain responses. (A) Paw withdraw threshold to mechanical stimuli on the ipsilateral hind paw at 3-, 7-, and 14 days post injury. Data represent Mean±SEM, N=8-10 per group, ***p<0.001 (SNI vs. sham), ###p<0.001 (SNI+boldine vs. SNI) by two-way ANOVA with Bonferroni post-tests; (B) Paw withdraw threshold to mechanical stimuli on the contralateral hind paw. (C) Withdraw latency to warm temperature (50°C) at 7 days post injury using a hot plate test apparatus (Maze Engineers). (D) Withdraw latency to cold temperature (15°C) at 7 days post injury using a cold plate test apparatus (Maze Engineers). Data represent Mean±SEM, N=8-10 per group, *p<0.05, **p<0.01, ***p<0.001 by one-way ANOVA with Tukey post-test.

Fig. 2 Effect of boldine on weight bearing following SNI. Assessment of spontaneous pain measuring the changes in postural equilibrium was achieved using the Dynamic Weight Bearing System 2.0 (Bioseb). (A) Weight support ratio of the ipsilateral hind limb vs. the contralateral hind limb; (B) Support area ratio of the ipsilateral hind limb vs. the contralateral hind limb; (C) Rearing duration; (D) Ipsilateral hind limb posed duration. Data represent Mean±SEM, N=8-10 per group, *p<0.05, **p<0.01, ***p<0.001, ****<p<0.0001 by two-way ANOVA with Tukey post-tests.

Fig. 3 Peripheral inflammation changes after SNI and boldine treatment. Serum samples collected at 15 dpi were subjected to a multiplex ELISA using the MILLIPLEX® Mouse Cytokine/Chemokine Magnetic Bead Panel (Millipore) and the median fluorescent intensity was used to calculate the concentration of each cytokine/chemokine. Data represent Mean±SEM, N=8-10 per group, *p<0.05, **p<0.01 by one-way ANOVA with Tukey post-test.

Fig. 4 Boldine decreased levels of reactive astrocytes and activated microglia after SNI. Sixteen micrometer thick transverse lumbar spinal cord sections were immuno-stained with astrocyte marker GFAP (Abcam, top panel) and activated microglia marker MHC II (Abcam, bottom panel) to evaluate the effect of SNI and boldine treatment on glia activation. Images displayed are representative examples from three mice per group. Images were acquired using the ZEISS LSM 700 confocal imaging system with 20× objective. Scale bar: 10 μm.

Fig. 5 Boldine decreased the expression of inflammation markers in the spinal cord. Total RNA was extracted from lumbar spinal cords collected at 15 dpi and subjected to gene expression

analysis. (A) TNF-α; (B) CCL2; (C) IL-1β mRNA levels were measured by quantitative PCR using standard Taqman methods. Relative levels were calculated using the $2^{-\Delta\Delta Ct}$ method with HPRT as an internal control. Data represent Mean±SEM, N=8-10 per group, *p<0.05, ***p<0.001 by t-test.

Fig. 6 Boldine inhibited LPS-induced inflammation in BV-2 microglial cells. BV-2 microglia cells were treated with 100 ng/ml lipopolysaccharides (LPS) with or without boldine (25 μg/ml or 50 μg/ml) for 6 hours. Cells were harvested and subjected to RNA extraction followed by cDNA synthesis and quantitative PCR using standard Taqman methods using probes including CCL2, CCL3, CCL5, CD11b, IL-1β, IL-6, IL-18, TNF-α, TLR2, TLR3, NLRP3, and caspase1 (all from Applied Biosystems). Data represent Mean±SEM, N=3 per condition, * p<0.05, **p<0.01, ***p<0.001, ****p<0.0001 by one-way ANOVA followed by Tukey posttests.

Fig. 7 Boldine inhibited LPS-induced inflammation in primary mouse astrocytes. Primary spinal cord astrocytes were generated from P2 C57BL6 mice. Astrocytes were treated with 100 ng/ml LPS with or without boldine (25 μg/ml or 50 μg/ml) for 6 hours. Cells were then harvested and subjected to RNA extraction followed by cDNA synthesis and quantitative PCR using standard Taqman methods using probes including CCL2, IL-1β, IL-6, IL-18, TNF-α, TLR2, TLR3, TLR6, NLRP3, caspase1, and NFκB (all from Applied Biosystems). Data represent Mean±SEM, N=3 per condition, * p<0.05, **p<0.01, ***p<0.001, ****p<0.0001 by one-way ANOVA followed by Tukey post-tests.

Conflict of Interest

Authors CAT, JCS, CPC, and WZ are co-inventors for US patent no. 11,707,459 for the use of boldine to treat neurological injuries. This study falls within the claims of the patent. The remaining authors declare that the research was conducted in the absence of any commercial or financial relationships that could be construed as a potential conflict of interest.

Author Contributions

JP collected data and performed analysis for all the experiments; YD and JCS designed and performed the molecular docking study; CC assisted analysis on behavioral tests; CAT assisted immunostaining; CPC assisted the study design and manuscript writing; WZ conceived and designed the study, collected data, performed analysis, and wrote the manuscript.

Funding

This study is supported by VA RR&D award I21RX003453 to WZ, VA TTP BRAVE award 2020-144 to WZ, VA RR&D award I50RX002020, ANID projects 1240695 to YD and 1231523 to JCS.

Acknowledgments

The authors would like to thank Dr. Miguel Gama-Sosa for helpful discussions related to technical aspects of the studies reported.

Abbreviations

ANOVA: Analysis of variance

BW: body weight

CCI: Chronic constriction injury

CCL: C-C Motif Chemokine Ligand

CXCL: C-X-C motif chemokine ligand

DMEM: Dulbecco's Modified Eagle Medium

Dpi: Days post injury

DWB: Dynamic Weight Bearing

ELISA: enzyme-linked immunosorbent assay

FBS: fetal bovine serum

GFAP: Glial fibrillary acidic protein

HPRT: Hypoxanthine phosphoribosyltransferase 1

IL: Interleukin

LPS: Lipopolysaccharides

M-CSF: macrophage-colony stimulating factor

MHC II: major histocompatibility complex II

NFκB: nuclear factor-kappa B

NLRP3: Nod-like receptor pyrin containing 3

NMDA: N-methyl-D-aspartate

NTH: N-terminal helix), and TMH2

PBS: phosphate-buffered saline

PFA: paraformaldehyde

SEM: standard error of the mean

SNI: Spared nerve injury

TMH: transmembrane helix

TNF-α: Tumor Necrosis Factor Alpha

TLR: Toll-like receptor

1. Colloca, L., et al., *Neuropathic pain*. Nat Rev Dis Primers, 2017. **3**: p. 17002.
2. Bair, M.J., et al., *Association of depression and anxiety alone and in combination with chronic musculoskeletal pain in primary care patients*. Psychosom Med, 2008. **70**(8): p. 890-7.
3. Descalzi, G., et al., *Neuropathic pain promotes adaptive changes in gene expression in brain networks involved in stress and depression*. Sci Signal, 2017. **10**(471).
4. Lerman, S.F., et al., *Longitudinal associations between depression, anxiety, pain, and pain-related disability in chronic pain patients*. Psychosom Med, 2015. **77**(3): p. 333-41.
5. McWilliams, L.A., R.D. Goodwin, and B.J. Cox, *Depression and anxiety associated with three pain conditions: results from a nationally representative sample*. Pain, 2004. **111**(1-2): p. 77-83.
6. Austin, P.J. and G. Moalem-Taylor, *The neuro-immune balance in neuropathic pain: involvement of inflammatory immune cells, immune-like glial cells and cytokines*. J Neuroimmunol, 2010. **229**(1-2): p. 26-50.
7. Ji, R.R., Z.Z. Xu, and Y.J. Gao, *Emerging targets in neuroinflammation-driven chronic pain*. Nat Rev Drug Discov, 2014. **13**(7): p. 533-48.
8. Kim, D., S. Lee, and S.J. Lee, *Toll-like receptors in peripheral nerve injury and neuropathic pain*. Curr Top Microbiol Immunol, 2009. **336**: p. 169-86.
9. Marchettini, P., et al., *Painful peripheral neuropathies*. Curr Neuropharmacol, 2006. **4**(3): p. 175-81.
10. Bernatoniene, J., et al., *Novel Drug Targets and Emerging Pharmacotherapies in Neuropathic Pain*. Pharmaceutics, 2023. **15**(7).
11. Finnerup, N.B., R. Kuner, and T.S. Jensen, *Neuropathic Pain: From Mechanisms to Treatment*. Physiol Rev, 2021. **101**(1): p. 259-301.
12. Abdelrahman, K.M. and K.V. Hackshaw, *Nutritional Supplements for the Treatment of Neuropathic Pain*. Biomedicines, 2021. **9**(6).

13. Sharma, S., et al., *Curcumin attenuates thermal hyperalgesia in a diabetic mouse model of neuropathic pain.* Eur J Pharmacol, 2006. **536**(3): p. 256-61.
14. Jeon, Y., et al., *Curcumin could prevent the development of chronic neuropathic pain in rats with peripheral nerve injury.* Curr Ther Res Clin Exp, 2013. **74**: p. 1-4.
15. Sáez, J.C., et al., *Pharmacology of boldine: summary of the field and update on recent advances.* Front Pharmacol, 2024. **15**: p. 1427147.
16. Speisky, H. and B.K. Cassels, *Boldo and boldine: an emerging case of natural drug development.* Pharmacol Res, 1994. **29**(1): p. 1-12.
17. O'Brien, P., C. Carrasco-Pozo, and H. Speisky, *Boldine and its antioxidant or health-promoting properties.* Chem Biol Interact, 2006. **159**(1): p. 1-17.
18. Backhouse, N., et al., *Anti-inflammatory and antipyretic effects of boldine.* Agents Actions, 1994. **42**(3-4): p. 114-7.
19. Catalan, M., et al., *Boldine prevents the inflammatory response of cardiac fibroblasts induced by SGK1-NFkappaB signaling pathway activation.* Cell Signal, 2024: p. 111241.
20. Toro, C.A., et al., *Boldine modulates glial transcription and functional recovery in a murine model of contusion spinal cord injury.* Front Cell Neurosci, 2023. **17**: p. 1163436.
21. Feng, J., et al., *Protective effect of Boldine against neuroinflammation in spinal cord injury in rats.* Israel Journal of Plant Sciences, 2021. **68**(1-2): p. 72-78.
22. Burrell, J.C., et al., *Orally administered boldine reduces muscle atrophy and promotes neuromuscular recovery in a rodent model of delayed nerve repair.* Front Cell Neurosci, 2023. **17**: p. 1240916.
23. Toledo, J.P., et al., *Boldine Attenuates Synaptic Failure and Mitochondrial Deregulation in Cellular Models of Alzheimer's Disease.* Front Neurosci, 2021. **15**: p. 617821.
24. Jimenez, I. and H. Speisky, *Biological disposition of boldine: in vitro and in vivo studies.* Phytother Res, 2000. **14**(4): p. 254-60.

25. Deuis, J.R., L.S. Dvorakova, and I. Vetter, *Methods Used to Evaluate Pain Behaviors in Rodents*. Front Mol Neurosci, 2017. **10**: p. 284.
26. Yalcin, I., et al., *Differentiating thermal allodynia and hyperalgesia using dynamic hot and cold plate in rodents*. J Pain, 2009. **10**(7): p. 767-73.
27. Segal, J.P., et al., *Weight bearing as a measure of disease progression in experimental autoimmune encephalomyelitis*. J Neuroimmunol, 2021. **361**: p. 577730.
28. Wang, J., et al., *Epigenetic modulation of inflammation and synaptic plasticity promotes resilience against stress in mice*. Nat. Commun, 2018. **9**(1): p. 477.
29. Wang, J., et al., *An Extract of Artemisia dracunculus L. Promotes Psychological Resilience in a Mouse Model of Depression*. Oxid Med Cell Longev, 2018. **2018**: p. 7418681.
30. Zhao, W., et al., *Peroxisome proliferator activator receptor gamma coactivator-1alpha (PGC-1alpha) improves motor performance and survival in a mouse model of amyotrophic lateral sclerosis*. Mol Neurodegener, 2011. **6**(1): p. 51.
31. Kerstetter, A.E. and R.H. Miller, *Isolation and culture of spinal cord astrocytes*. Methods Mol Biol, 2012. **814**: p. 93-104.
32. Lee, H.J., et al., *Conformational changes in the human Cx43/GJA1 gap junction channel visualized using cryo-EM*. Nat Commun, 2023. **14**(1): p. 931.
33. Halgren, T.A., et al., *Glide: a new approach for rapid, accurate docking and scoring. 2. Enrichment factors in database screening*. J Med Chem, 2004. **47**(7): p. 1750-9.
34. Guo, A., et al., *Inhibition of connexin hemichannels alleviates neuroinflammation and hyperexcitability in temporal lobe epilepsy*. Proc Natl Acad Sci U S A, 2022. **119**(45): p. e2213162119.
35. Challa, S.R., *Surgical animal models of neuropathic pain: Pros and Cons*. Int J Neurosci, 2015. **125**(3): p. 170-4.
36. Decosterd, I. and C.J. Woolf, *Spared nerve injury: an animal model of persistent peripheral neuropathic pain*. Pain, 2000. **87**(2): p. 149-158.

37. Nothem, M.A., et al., *Effects of ethanol on mechanical allodynia and dynamic weight bearing in male and female mice with spared nerve injury.* Alcohol Clin Exp Res (Hoboken), 2023. **47**(2): p. 382-394.
38. Cheng, T., Z. Xu, and X. Ma, *The role of astrocytes in neuropathic pain.* Frontiers in Molecular Neuroscience, 2022. **15**.
39. Lu, H.J. and Y.J. Gao, *Astrocytes in Chronic Pain: Cellular and Molecular Mechanisms.* Neurosci Bull, 2023. **39**(3): p. 425-439.
40. Inoue, K. and M. Tsuda, *Microglia in neuropathic pain: cellular and molecular mechanisms and therapeutic potential.* Nature Reviews Neuroscience, 2018. **19**(3): p. 138-152.
41. Karavis, M.Y., et al., *Role of Microglia in Neuropathic Pain.* Cureus, 2023. **15**(8): p. e43555.
42. Chen, G., et al., *Connexin-43 induces chemokine release from spinal cord astrocytes to maintain late-phase neuropathic pain in mice.* Brain, 2014. **137**(Pt 8): p. 2193-209.
43. Hanisch, U.K., *Microglia as a source and target of cytokines.* Glia, 2002. **40**(2): p. 140-55.
44. Milligan, E.D., et al., *Spinal glia and proinflammatory cytokines mediate mirror-image neuropathic pain in rats.* J Neurosci, 2003. **23**(3): p. 1026-40.
45. Gui, W.S., et al., *Interleukin-1beta overproduction is a common cause for neuropathic pain, memory deficit, and depression following peripheral nerve injury in rodents.* Mol Pain, 2016. **12**.
46. Biber, K. and E. Boddeke, *Neuronal CC chemokines: the distinct roles of CCL21 and CCL2 in neuropathic pain.* Front Cell Neurosci, 2014. **8**: p. 210.
47. Ma, S.B., et al., *CCL2 facilitates spinal synaptic transmission and pain via interaction with presynaptic CCR2 in spinal nociceptor terminals.* Mol Brain, 2020. **13**(1): p. 161.

48. Van Steenwinckel, J., et al., *CCL2 released from neuronal synaptic vesicles in the spinal cord is a major mediator of local inflammation and pain after peripheral nerve injury.* J Neurosci, 2011. **31**(15): p. 5865-75.
49. Leybaert, L., et al., *Connexins in Cardiovascular and Neurovascular Health and Disease: Pharmacological Implications.* Pharmacol Rev, 2017. **69**(4): p. 396-478.
50. Yi, C., et al., *Inhibition of glial hemichannels by boldine treatment reduces neuronal suffering in a murine model of Alzheimer's disease.* Glia, 2017. **65**(10): p. 1607-1625.
51. Li, H., et al., *The connexin hemichannel inhibitor D4 produces rapid antidepressant-like effects in mice.* J Neuroinflammation, 2023. **20**(1): p. 191.
52. Guida, F., et al., *Behavioral, Biochemical and Electrophysiological Changes in Spared Nerve Injury Model of Neuropathic Pain*. Int J Mol Sci, 2020. **21**(9).
53. Sheehan, G.D., et al., *Thermal hyperalgesia and dynamic weight bearing share similar recovery dynamics in a sciatic nerve entrapment injury model.* Neurobiol Pain, 2021. **10**: p. 100079.
54. Wolter, A., et al., *Evaluating rearing behaviour as a model-specific pain indicator in mouse osteotomy models.* Lab Anim, 2024. **58**(1): p. 9-21.
55. Ji, R.R., T. Berta, and M. Nedergaard, *Glia and pain: is chronic pain a gliopathy?* Pain, 2013. **154 Suppl 1**(0 1): p. S10-S28.
56. Bradesi, S., *Role of spinal cord glia in the central processing of peripheral pain perception*. Neurogastroenterol Motil, 2010. **22**(5): p. 499-511.
57. Leyh, J., et al., *Classification of Microglial Morphological Phenotypes Using Machine Learning*. Frontiers in Cellular Neuroscience, 2021. **15**.
58. Ji, R.R., A. Chamessian, and Y.Q. Zhang, *Pain regulation by non-neuronal cells and inflammation*. Science, 2016. **354**(6312): p. 572-577.
59. Jiang, B.C., T. Liu, and Y.J. Gao, *Chemokines in chronic pain: cellular and molecular mechanisms and therapeutic potential.* Pharmacol Ther, 2020. **212**: p. 107581.
60. Binshtok, A.M., et al., *Nociceptors are interleukin-1beta sensors.* J Neurosci, 2008. **28**(52): p. 14062-73.

61. Helyes, Z., et al., *Transfer of complex regional pain syndrome to mice via human autoantibodies is mediated by interleukin-1-induced mechanisms.* Proc Natl Acad Sci U S A, 2019. **116**(26): p. 13067-13076.

62. Wang, X.B., et al., *A novel primary culture method for high-purity satellite glial cells derived from rat dorsal root ganglion.* Neural Regen Res, 2019. **14**(2): p. 339-345.

63. Safieh-Garabedian, B., et al., *Contribution of interleukin-1 beta to the inflammation-induced increase in nerve growth factor levels and inflammatory hyperalgesia.* Br J Pharmacol, 1995. **115**(7): p. 1265-75.

64. Dean, N.J., et al., *Anti-IL-5 biologics and rheumatoid arthritis: a single-centre 500 patient year exposure analysis.* RMD Open, 2023. **9**(4).

65. Merriwether, E.N., et al., *IL-5 mediates monocyte phenotype and pain outcomes in fibromyalgia.* Pain, 2021. **162**(5): p. 1468-1482.

66. Verri, W.A., Jr., et al., *Nociceptive effect of subcutaneously injected interleukin-12 is mediated by endothelin (ET) acting on ETB receptors in rats.* J Pharmacol Exp Ther, 2005. **315**(2): p. 609-15.

67. Gomez-Nicola, D., et al., *Role of IL-15 in spinal cord and sciatic nerve after chronic constriction injury: regulation of macrophage and T-cell infiltration.* J Neurochem, 2008. **107**(6): p. 1741-52.

68. Warner, S.C., et al., *IL-15 and IL15RA in Osteoarthritis: Association With Symptoms and Protease Production, but Not Structural Severity.* Front Immunol, 2020. **11**: p. 1385.

69. Liou, J.T., et al., *Peritoneal administration of Met-RANTES attenuates inflammatory and nociceptive responses in a murine neuropathic pain model.* J Pain, 2013. **14**(1): p. 24-35.

70. Zhang, Y., et al., *A transcriptomic analysis of neuropathic pain in the anterior cingulate cortex after nerve injury.* Bioengineered, 2022. **13**(2): p. 2058-2075.

71. Karl-Scholler, F., et al., *A translational study: Involvement of miR-21-5p in development and maintenance of neuropathic pain via immune-related targets CCL5 and YWHAE.* Exp Neurol, 2022. **347**: p. 113915.

72. Lechner, J. and V. von Baehr, *Peripheral Neuropathic Facial/Trigeminal Pain and RANTES/CCL5 in Jawbone Cavitation*. Evid Based Complement Alternat Med, 2015. **2015**: p. 582520.
73. Grad, S., et al., *Systemic blood plasma CCL5 and CXCL6: Potential biomarkers for human lumbar disc degeneration*. Eur Cell Mater, 2016. **31**: p. 1-10.
74. Kepler, C.K., et al., *Expression and relationship of proinflammatory chemokine RANTES/CCL5 and cytokine IL-1beta in painful human intervertebral discs*. Spine (Phila Pa 1976), 2013. **38**(11): p. 873-80.
75. Baldimtsi, E., et al., *The role of chemokines in type 1 diabetes-associated neuropathy*. Endocrinol Diabetes Metab, 2023. **6**(3): p. e419.
76. Piotrowska, A., et al., *Pharmacological blockade of CXCR3 by (+/-)-NBI-74330 reduces neuropathic pain and enhances opioid effectiveness - Evidence from in vivo and in vitro studies*. Biochim Biophys Acta Mol Basis Dis, 2018. **1864**(10): p. 3418-3437.
77. Yu, X., A. Basbaum, and Z. Guan, *Contribution of colony-stimulating factor 1 to neuropathic pain*. Pain Rep, 2021. **6**(1): p. e883.
78. Collison, J., *CSF1 drives pain in arthritis*. Nat Rev Rheumatol, 2018. **14**(10): p. 562.
79. Watkins, L.R. and S.F. Maier, *Glia: a novel drug discovery target for clinical pain*. Nat Rev Drug Discov, 2003. **2**(12): p. 973-85.
80. Li, Y., et al., *The Cancer Chemotherapeutic Paclitaxel Increases Human and Rodent Sensory Neuron Responses to TRPV1 by Activation of TLR4*. J Neurosci, 2015. **35**(39): p. 13487-500.
81. Tanga, F.Y., N. Nutile-McMenemy, and J.A. DeLeo, *The CNS role of Toll-like receptor 4 in innate neuroimmunity and painful neuropathy*. Proc Natl Acad Sci U S A, 2005. **102**(16): p. 5856-61.
82. Hanamsagar, R., M.L. Hanke, and T. Kielian, *Toll-like receptor (TLR) and inflammasome actions in the central nervous system*. Trends Immunol, 2012. **33**(7): p. 333-42.
83. Schroder, K. and J. Tschopp, *The inflammasomes*. Cell, 2010. **140**(6): p. 821-32.

84. Tonkin, R.S., et al., *Attenuation of mechanical pain hypersensitivity by treatment with Peptide5, a connexin-43 mimetic peptide, involves inhibition of NLRP3 inflammasome in nerve-injured mice*. Exp Neurol, 2018. **300**: p. 1-12.

85. Jeanson, T., et al., *Potentiation of Amitriptyline Anti-Hyperalgesic-Like Action By Astroglial Connexin 43 Inhibition in Neuropathic Rats*. Sci Rep, 2016. **6**: p. 38766.

Figure 1

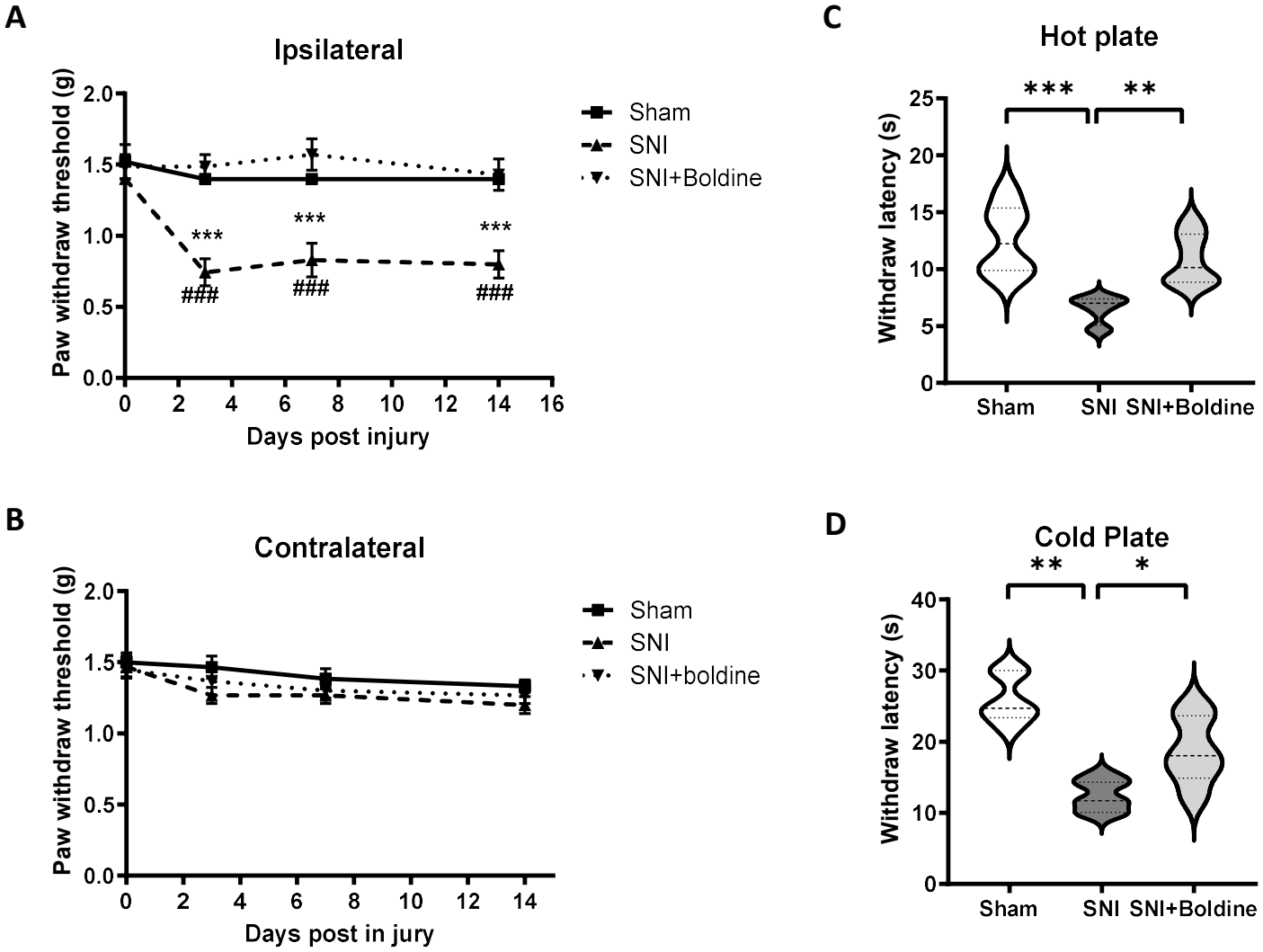
A
Ipsilateral
Paw withdraw threshold (g)
2.0
1.5
1.0
0.5
0.0
0
2
4
6
8
10
12
14
16
Days post injury
***
***
***
###
###
###
Sham
SNI
SNI+Boldine
B
Contralateral
Paw withdraw threshold (g)
2.0
1.5
1.0
0.5
0.0
0
2
4
6
8
10
12
14
Days post in jury
Sham
SNI
SNI+boldine
C
Hot plate
Withdraw latency (s)
25
20
15
10
5
0
***
**
Sham
SNI
SNI+Boldine
D
Cold Plate
Withdraw latency (s)
40
30
20
10
0
**
*
Sham
SNI
SNI+Boldine

Figure 2

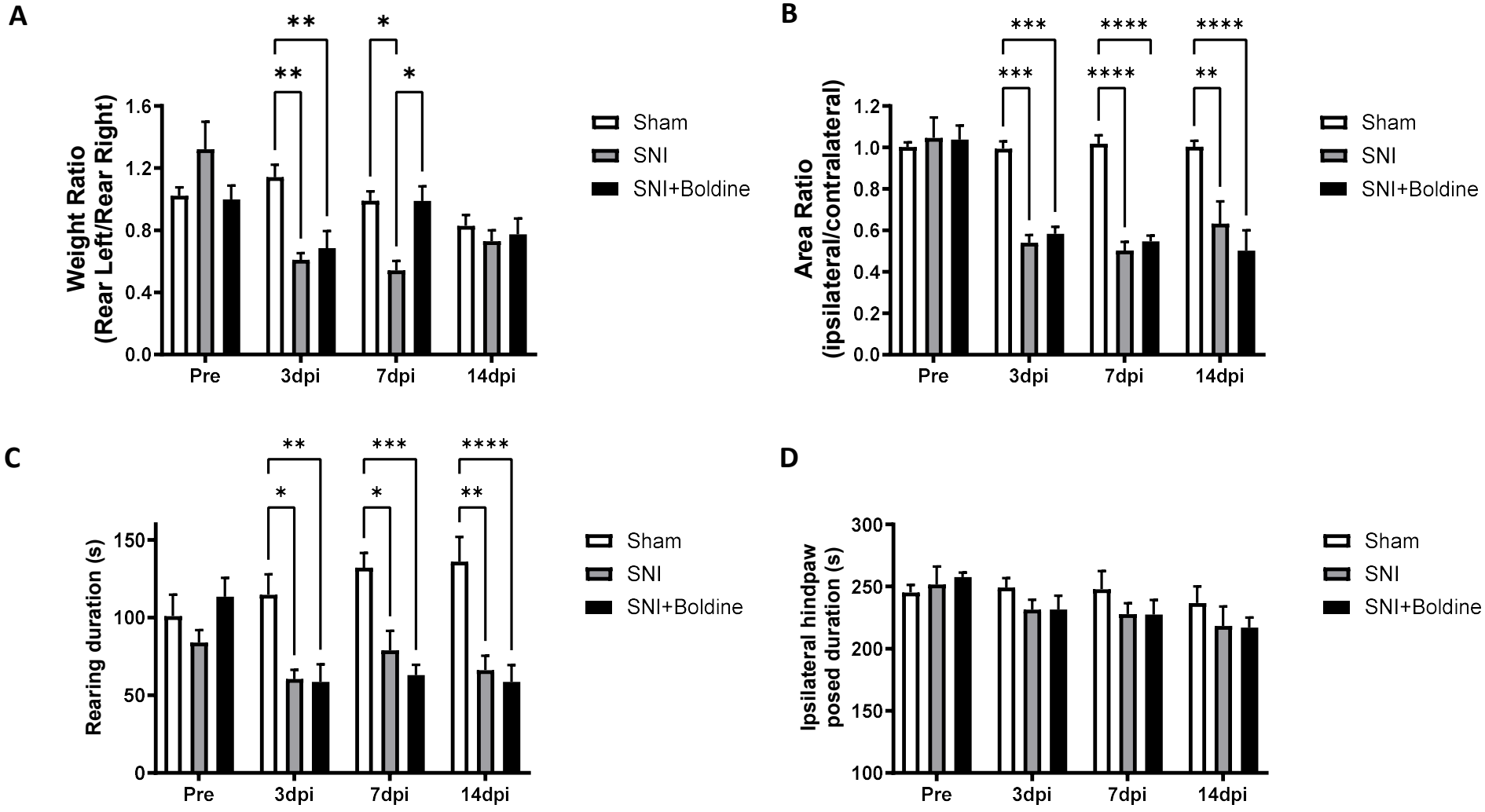
A
Weight Ratio
(Rear Left/Rear Right)
1.6
1.2
0.8
0.4
0.0
Pre
3dpi
7dpi
14dpi
**
**
*
*
Sham
SNI
SNI+Boldine
B
Area Ratio
(ipsilateral/contralateral)
1.2
1.0
0.8
0.6
0.4
0.2
0.0
Pre
3dpi
7dpi
14dpi
***
***
****
****
****
**
Sham
SNI
SNI+Boldine
C
Rearing duration (s)
150
100
50
0
Pre
3dpi
7dpi
14dpi
**
*
***
*
****
**
Sham
SNI
SNI+Boldine
D
Ipsilateral hindpaw
posed duration (s)
300
250
200
150
100
Pre
3dpi
7dpi
14dpi
Sham
SNI
SNI+Boldine

Figure 3

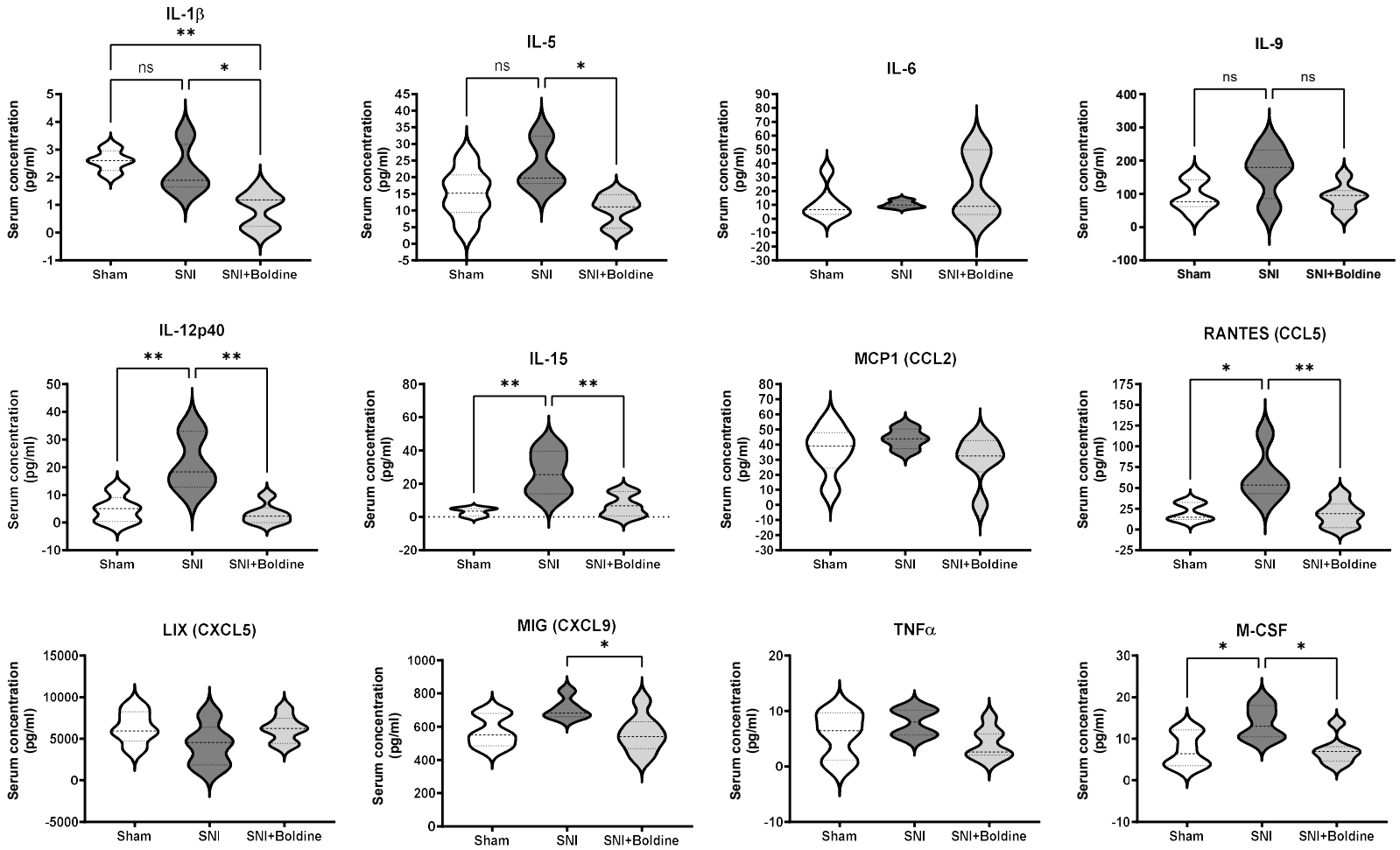
IL-1β
**
ns
*
IL-5
ns
*
IL-6
IL-9
ns
ns
IL-12p40
**
**
IL-15
**
**
MCP1 (CCL2)
RANTES (CCL5)
*
**
LIX (CXCL5)
MIG (CXCL9)
*
TNFα
M-CSF
*
*
Serum concentration (pg/ml)
Sham
SNI
SNI+Boldine

Figure 4

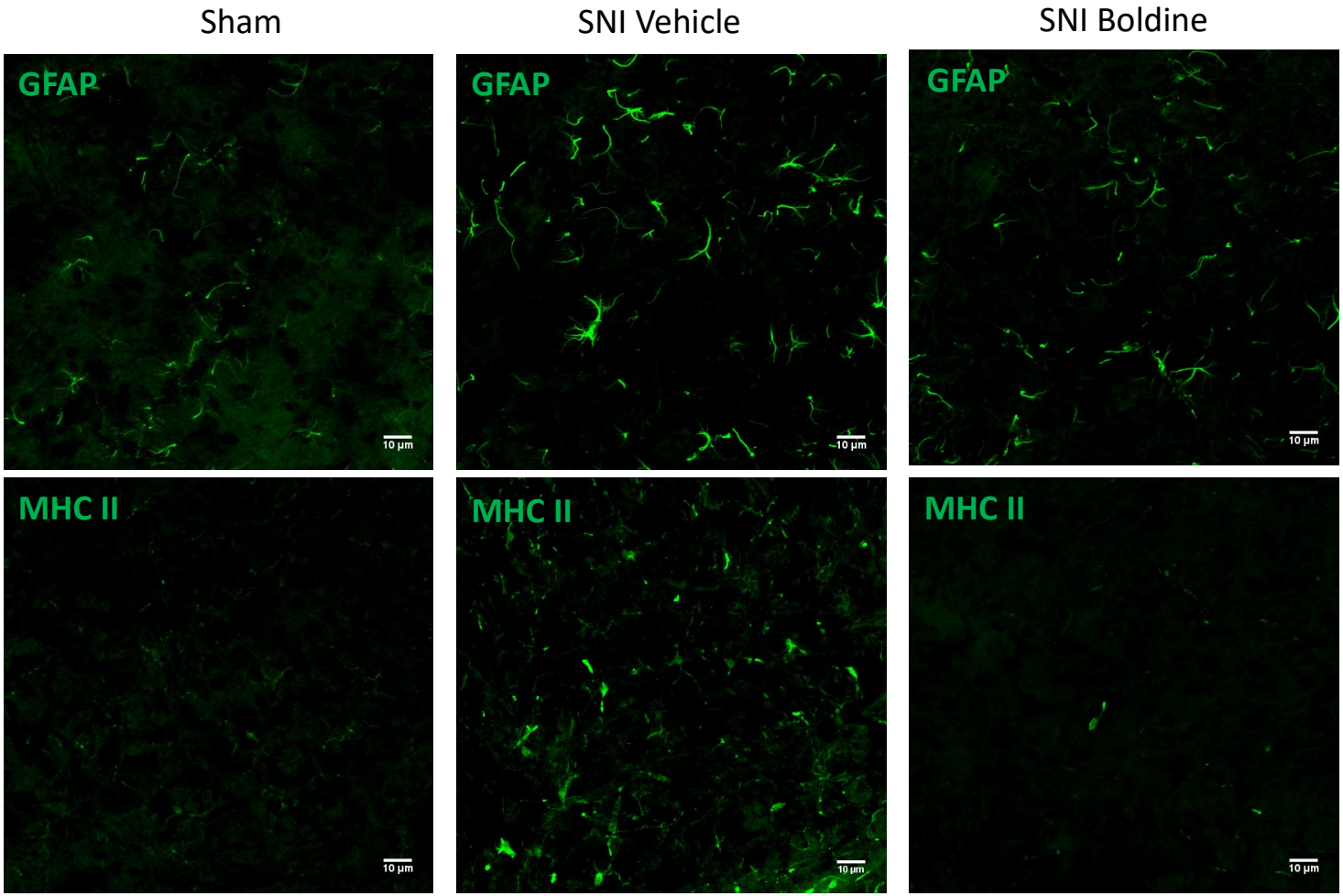
Sham
SNI Vehicle
SNI Boldine
GFAP
GFAP
GFAP
MHC II
MHC II
MHC II
10 µm

Figure 5

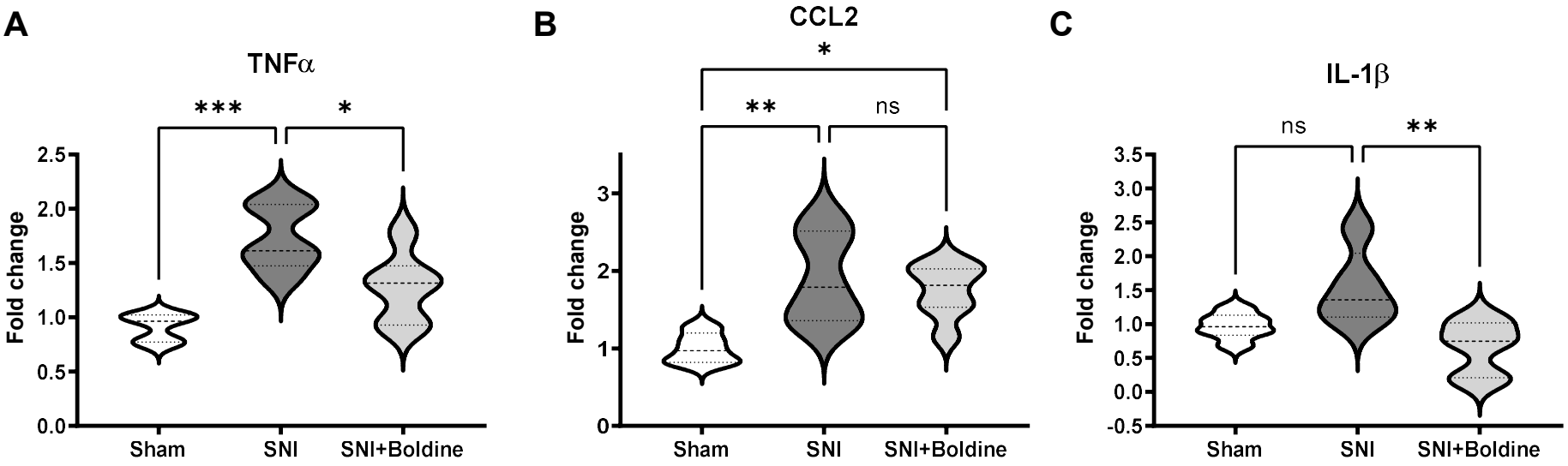
A
TNFα
***
*
Fold change
2.5
2.0
1.5
1.0
0.5
0.0
Sham
SNI
SNI+Boldine
B
CCL2
*
**
ns
Fold change
3
2
1
0
Sham
SNI
SNI+Boldine
C
IL-1β
ns
**
Fold change
3.5
3.0
2.5
2.0
1.5
1.0
0.5
0.0
-0.5
Sham
SNI
SNI+Boldine

Figure 6

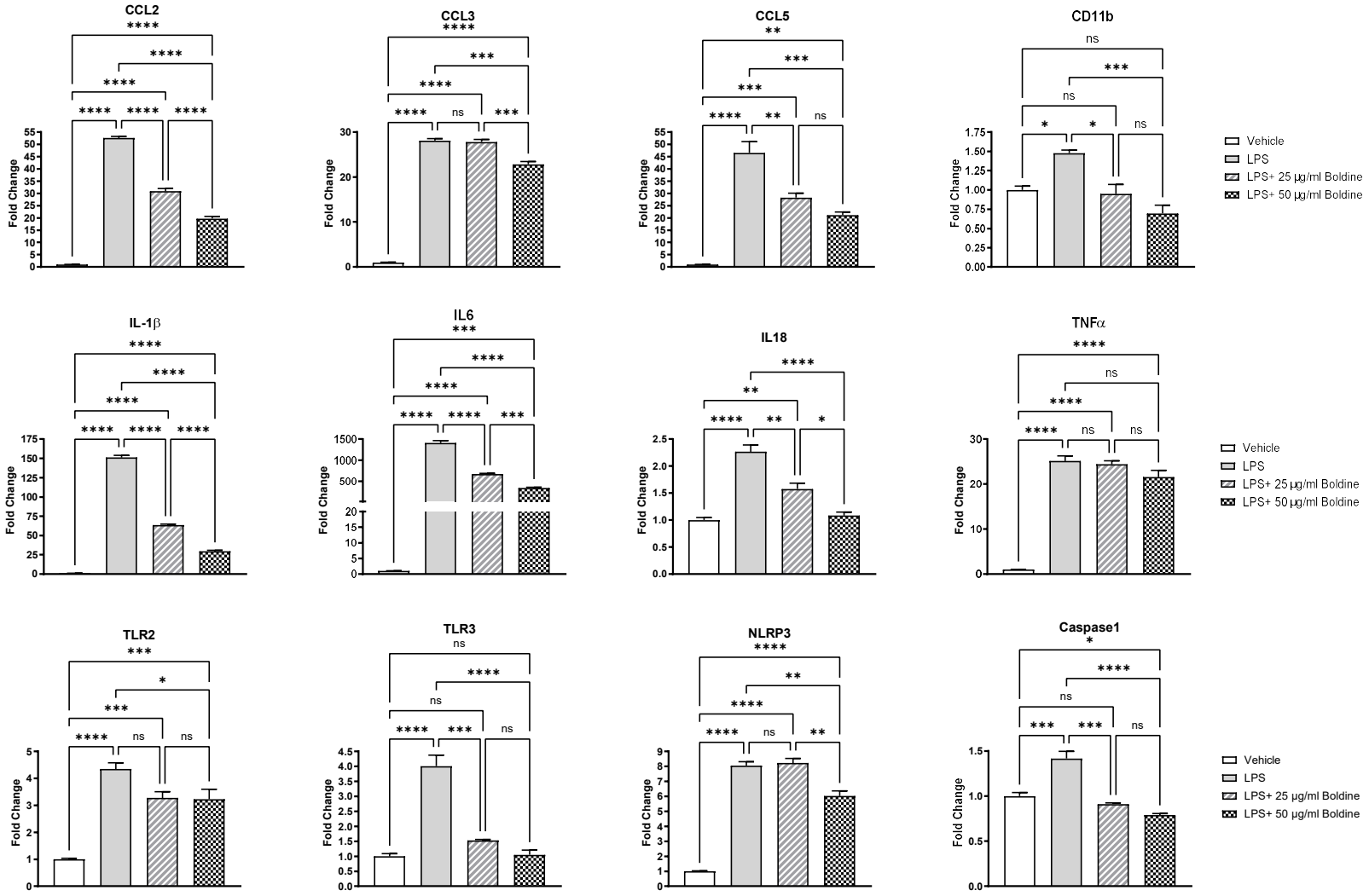
CCL2
CCL3
CCL5
CD11b
IL-1β
IL6
IL18
TNFα
TLR2
TLR3
NLRP3
Caspase1
Fold Change
Vehicle
LPS
LPS+ 25 μg/ml Boldine
LPS+ 50 μg/ml Boldine

Figure 7

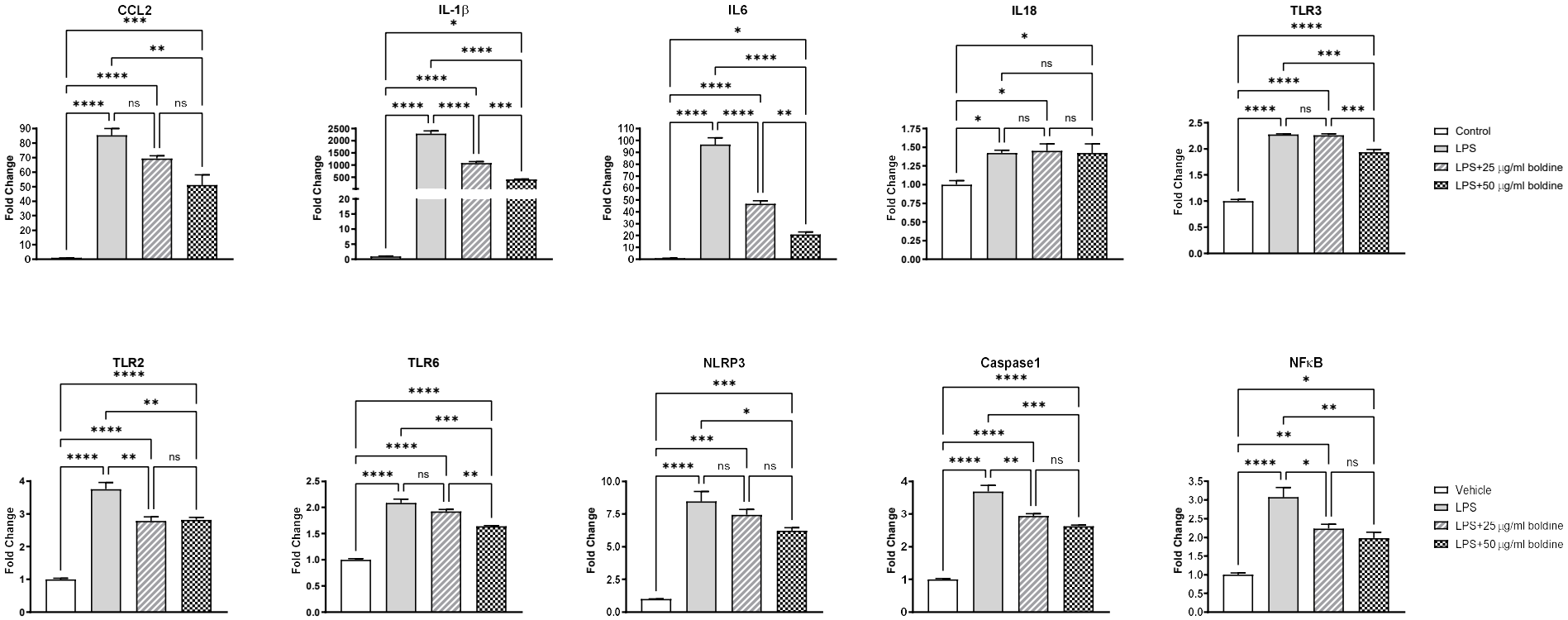
CCL2
IL-1β
IL6
IL18
TLR3
TLR2
TLR6
NLRP3
Caspase1
NFκB
Fold Change
Control
LPS
LPS+25 μg/ml boldine
LPS+50 μg/ml boldine
Vehicle
LPS
LPS+25 μg/ml boldine
LPS+50 μg/ml boldine